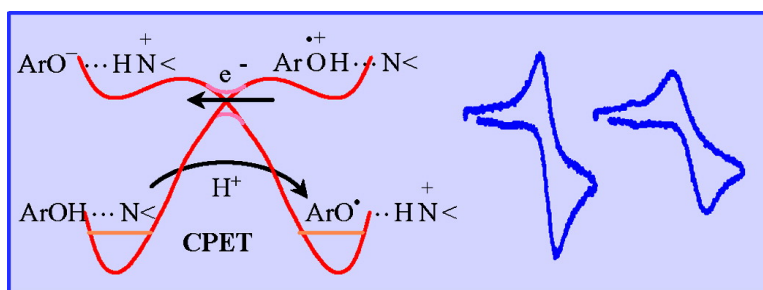


## Adiabatic and Non-adiabatic Concerted Proton–Electron Transfers. Temperature Effects in the Oxidation of Intramolecularly Hydrogen-Bonded Phenols

Cyrille Costentin, Marc Robert, and Jean-Michel Savant

*J. Am. Chem. Soc.*, **2007**, 129 (32), 9953–9963 • DOI: 10.1021/ja071150d • Publication Date (Web): 19 July 2007

Downloaded from <http://pubs.acs.org> on February 15, 2009



### More About This Article

Additional resources and features associated with this article are available within the HTML version:

- Supporting Information
- Links to the 13 articles that cite this article, as of the time of this article download
- Access to high resolution figures
- Links to articles and content related to this article
- Copyright permission to reproduce figures and/or text from this article

[View the Full Text HTML](#)

## Adiabatic and Non-adiabatic Concerted Proton–Electron Transfers. Temperature Effects in the Oxidation of Intramolecularly Hydrogen-Bonded Phenols

Cyrille Costentin, Marc Robert, and Jean-Michel Savéant\*

Contribution from the Laboratoire d'Electrochimie Moléculaire, Unité Mixte de Recherche  
Université - CNRS No. 7591, Université Paris Diderot,  
2 place Jussieu, 75251 Paris Cedex 05, France

Received February 16, 2007; E-mail: saveant@univ-paris-diderot.fr

**Abstract:** The one-electron electrochemical and homogeneous oxidations of two closely similar aminophenols that undergo a concerted proton–electron transfer reaction, in which the phenolic proton is transferred to the nitrogen atom in concert with electron transfer, are taken as examples to test procedures that allow the separate determination of the degree of adiabaticity and the reorganization energy of the reaction. The Marcus (or Marcus–Hush–Levich) formalism is applicable in both cases, but not necessarily in its adiabatic version. Linearization of the activation–driving force laws simplifies the treatment of the kinetic data, notably allowing the use of Arrhenius plots to treat the temperature dependence of the rate constant. A correct estimation of the adiabaticity and reorganization energy requires the determination of the variation of the driving force with temperature. Application of these procedures led to the conclusion that, unlike previous reports, the homogeneous reaction is non-adiabatic, with a transmission coefficient of the order of 0.005, and that the self-exchange reorganization energy is about 1 eV lower than previously estimated. With such systems, the intramolecular reorganization energy, although sizable, is in fact rather modest, being only slightly larger than that for the outer-sphere electron transfer that produced the cation radical. The electrochemical reaction is, in contrast, adiabatic, as revealed by the temperature dependence of its standard rate constant obtained from cyclic voltammetric experiments. This difference in behavior is deemed to derive from the effect of the strong electric field within which the electrochemical reaction takes place, stabilizing a zwitterionic form of the reactant (in which the proton has been transferred from oxygen to nitrogen). Taking this difference in adiabaticity into account, the magnitudes of the reorganization energies of the two reactions appear to be quite compatible with one another, as revealed by an analysis of the solvent and intramolecular contributions in both cases.

### Introduction

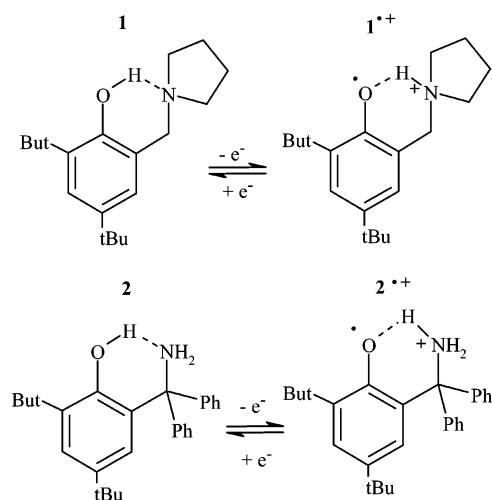
The mechanisms and kinetics of proton-coupled electron transfers (PCET), where proton and electron transfer involves different molecular centers, currently attract active attention as fundamental problems of chemical reactivity, bolstered by the involvement of PCET in many natural processes.<sup>1</sup> Particular emphasis has been put on the possibility that the two steps be concerted, giving rise to concerted proton–electron transfer (CPET) reactions. Several homogeneous<sup>2–5</sup> or electrochemical<sup>6–9</sup> systems have been investigated with a view toward illustrating the occurrence of CPET pathways, rather than the competing

stepwise pathways that involve the transfer of an electron followed by the transfer of a proton and/or the reverse sequence.

- (1) (a) Stubbe, J.; van der Donk, W. A. *Chem. Rev.* **1998**, *98*, 705. (b) Stubbe, J.; Nocera, D. G.; Yee, C. S.; Chang, M. C. Y. *Chem. Rev.* **2003**, *103*, 2167. (c) Chang, C. J.; Chang, M. C. Y.; Damrauer, N. H.; Nocera, D. G. *Biochim. Biophys. Acta* **2004**, *1655*, 13. (d) Renger, G. *Biochim. Biophys. Acta* **2004**, *1655*, 195. (e) McEvoy, J. P.; Brudvig, G. W. *Phys. Chem. Chem. Phys.* **2004**, *6*, 4754.
- (2) (a) Seyedsayamdost, M. R.; Yee, C. S.; Reece, S. Y.; Nocera, D. G.; Stubbe, J. *J. Am. Chem. Soc.* **2006**, *128*, 1562. (b) Seyedsayamdost, M. R.; Reece, S. Y.; Nocera, D. G.; Stubbe, J. *J. Am. Chem. Soc.* **2006**, *128*, 1569.
- (3) (a) Rhile, I. J.; Mayer, J. M. *Biochem. Biophys. Acta* **2004**, *1655*, 51. (b) Rhile, I. J.; Mayer, J. M. *J. Am. Chem. Soc.* **2004**, *126*, 12718. (c) Rhile, I. J.; Markle, T. F.; Nagao, H.; DiPasquale, A. G.; Lam, O. P.; Lockwood, M. A.; Rotter, K.; Mayer, J. M. *J. Am. Chem. Soc.* **2006**, *128*, 6075.

- (4) (a) Binstead, R. A.; Meyer, T. J. *J. Am. Chem. Soc.* **1987**, *109*, 3287. (b) Huynh, M. H. V.; Meyer, T. J. *Proc. Natl. Acad. Sci. U.S.A.* **2004**, *101*, 13138. (c) Fecenko, C. J.; Meyer, T. J.; Thorp, H. H. *J. Am. Chem. Soc.* **2006**, *128*, 11020. (d) Biczók, L.; Gupta, N.; Linschitz, H. *J. Am. Chem. Soc.* **1997**, *119*, 12601. (e) Gupta, N.; Linschitz, H. *J. Am. Chem. Soc.* **1997**, *119*, 6384. (f) Shukla, D.; Young, R. H.; Farid, S. *J. Phys. Chem. A* **2004**, *108*, 10386.
- (5) (a) Sjödin, M.; Styring, S.; Åkermark, B.; Sun, L.; Hammarström, L. *J. Am. Chem. Soc.* **2000**, *122*, 3932. (b) Sjödin, M.; Styring, S.; Åkermark, B.; Sun, L.; Hammarström, L. *Philos. Trans. R. Soc. London, Ser. B* **2002**, *357*, 1471. (c) Sjödin, M.; Ghanem, R.; Polivka, T.; Pan, J.; Styring, S.; Sun, L.; Sundström, V.; Hammarström, L. *Phys. Chem. Chem. Phys.* **2004**, *6*, 4851. (d) Sjödin, M.; Styring, S.; Wolpher, H.; Xu, Y.; Sun, L.; Hammarström, L. *J. Am. Chem. Soc.* **2005**, *127*, 3855. (e) Sjödin, M.; Irebo, T.; Utas, J. E.; Lind, J.; Merenyi, G.; Åkermark, B.; Hammarström, L. *J. Am. Chem. Soc.* **2006**, *128*, 13076.
- (6) (a) Costentin, C.; Evans, D. H.; Robert, M.; Savéant, J.-M.; Singh, P. S. *J. Am. Chem. Soc.* **2005**, *127*, 12490. (b) Singh, P. S.; Evans, D. H. *J. Phys. Chem. B* **2006**, *110*, 637.
- (7) (a) Haddox, R. M.; Finklea, H. O. *J. Phys. Chem. B* **2004**, *108*, 1694. (b) Madhiri, N.; Finklea, H. O. *Langmuir* **2006**, *22*, 10643.
- (8) (a) Costentin, C.; Robert, M.; Savéant, J.-M. *J. Am. Chem. Soc.* **2006**, *128*, 4552. (b) Costentin, C.; Robert, M.; Savéant, J.-M. *J. Am. Chem. Soc.* **2006**, *128*, 8726.
- (9) Macias-Ruvalcaba, N. A.; Okumura, N.; Evans, D. H. *J. Phys. Chem. B* **2006**, *110*, 22043.

## Scheme 1



In most analyses of experimental homogeneous CPET reactions, use of the Marcus theory, originally devised for outer-sphere electron transfers in its adiabatic version,<sup>10</sup> has been preferred<sup>3,5</sup> to the application of treatments specifically designed for CPET reactions,<sup>11–14</sup> for the reason that these treatments require the knowledge of several not-easily-accessible parameters. In the electrochemical case, it has been shown that, depending on a few simplifying assumptions, the Marcus–Hush–Levich (MHL) treatment of outer-sphere electrochemical electron transfer can be applied to CPET.<sup>15</sup> To what extent such a simplified approach is justified is a question that we discuss below, taking as example the one-electron electrochemical and homogeneous oxidation of a phenol coupled with an intramolecular amine-driven proton transfer. Coupled to the issue of the validity of MHL approach in the electrochemical case (or Marcus theory in the homogeneous case) is the question of the degree of adiabaticity of the reaction. The resolution of this problem requires a separate determination of the pre-exponential factor and the reorganization energy, calling for an examination of the rate constant variations with temperature. In the electrochemical case, this is derived from the variation of the cyclic

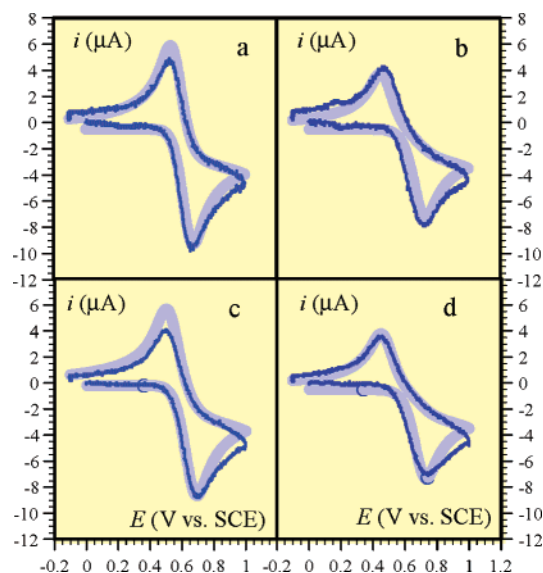


**Figure 1.** Cyclic voltammetry of **1** (2.5 mM) at a glassy carbon electrode in acetonitrile + 0.1 M *n*-NBu<sub>4</sub>PF<sub>6</sub> (a,b) or in acetonitrile + 0.1 M *n*-NBu<sub>4</sub>PF<sub>6</sub> + 2% CD<sub>3</sub>OD (c,d). Thin lines, experiments; bold line, simulations (see text). Scan rate, 0.5 V/s; temperature, 10 °C (a,c) or –10 °C (b,d).

voltammogram with temperature. These are the results that we describe first with the example of the phenol denoted **1** (Scheme 1). In the homogeneous case, we make use of previous results obtained for the oxidation of a very similar phenol, denoted **2** (Scheme 1), by a series of arylamine cation radicals<sup>3c</sup> that we have completed by a temperature-dependent cyclic voltammetric study aiming at the determination of the standard entropy of the oxidation reaction. These results form the basis of the following discussion of the two abovementioned issues.

## Results and Discussion

### 1. Electrochemical Oxidation of Compound 1.

**1.1. Variations with Temperature.** Examples of cyclic voltammograms of **1** in acetonitrile obtained at 10 and –10 °C are shown in Figure 1a,b. The anodic-to-cathodic peak separation increases as the temperature is decreased, indicating a slowdown of the reaction. The cyclic voltammograms recorded at other temperatures between –20 and 20 °C are available in the Supporting Information (Figure 1S). The hydrogen/deuterium isotope effect appears in Figures 1c,d, where the two preceding experiments have been repeated in the presence of 2% CD<sub>3</sub>OD. The cyclic voltammograms recorded at other temperatures in the same medium are also available in the Supporting Information (Figure 1S).<sup>16</sup>

As a first approximation, we may treat the results in Figure 1 and those displayed in the Supporting Information by means of the empirical Butler–Volmer kinetic law, which relates the current density to the potential according to eq 1,

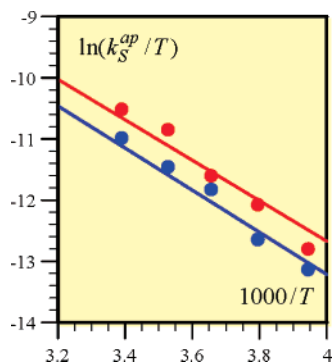
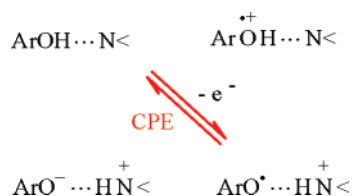
$$\frac{i}{i^0} = -k_S^{\text{ap}} \exp\left[\frac{\alpha F}{RT}(E - E^0)\right] \left\{ [1]_0 - \exp\left[-\frac{F}{RT}(E - E^0)\right] [1^{*+}]_0 \right\} \quad (1)$$

(16) The waves are not perfectly reversible at the highest temperatures because of a slight instability of the cation radical toward deprotonation, as already noted from the effect of scan rate.<sup>8a</sup>

- (10) (a) Marcus, R. A.; Sutin, N. *Biochim. Biophys. Acta* **1985**, *811*, 265. (b) Marcus, R. A. *J. Phys. Chem.* **1963**, *67*, 853.
- (11) (a) Cukier, R. I. *J. Phys. Chem.* **1996**, *100*, 15428. (b) Cukier, R. I.; Nocera, D. G. *Annu. Rev. Phys. Chem.* **1998**, *49*, 337. (c) Cukier, R. I. *J. Phys. Chem. A* **1999**, *103*, 5989. (d) Cukier, R. I. *J. Phys. Chem. B* **2002**, *106*, 1746. (e) Cukier, R. I. *Biochim. Biophys. Acta, Bioenerg.* **2004**, *1655*, 37.
- (12) (a) Soudackov, A.; Hammes-Schiffer, S. *J. Chem. Phys.* **1999**, *111*, 4672. Soudackov, A.; Hammes-Schiffer, S. *J. Chem. Phys.* **2000**, *113*, 2385. (b) Jordanova, N.; Decornez, H.; Hammes-Schiffer, S. *J. Am. Chem. Soc.* **2001**, *123*, 3723. (c) Hammes-Schiffer, S. *Acc. Chem. Res.* **2001**, *34*, 273. (d) Hammes-Schiffer, S. Proton-coupled electron transfer. In *Electron Transfer in Chemistry Vol. 1: Principles, Theories, Methods, and Techniques*; Balzani, V., Ed.; Wiley-VCH: Weinheim, Germany, 2001. (e) Jordanova, N.; Hammes-Schiffer, S. *J. Am. Chem. Soc.* **2002**, *124*, 4848. (f) Webb, S. P.; Jordanov, T.; Hammes-Schiffer, S. *J. Chem. Phys.* **2002**, *117*, 4106. (g) Pak, M. V.; Swalina, C.; Webb, S. P.; Hammes-Schiffer, S. *Chem. Phys.* **2004**, *304*, 227. (h) Hammes-Schiffer, S.; Jordanova, N. *Biochim. Biophys. Acta, Bioenerg.* **2004**, *1655*, 29. (i) Hatcher, E.; Soudackov, A.; Hammes-Schiffer, S. *J. Phys. Chem. B* **2005**, *109*, 18565. (j) Soudackov, A.; Hatcher, E.; Hammes-Schiffer, S. *J. Chem. Phys.* **2005**, *122*, 014505. (k) Hatcher, E.; Soudackov, A.; Hammes-Schiffer, S. *Chem. Phys.* **2005**, *319*, 93. (l) Hammes-Schiffer, S. Proton-coupled electron transfer reactions: Theoretical formulation and applications. In *Handbook of Hydrogen Transfer. Vol. 1: Physical and Chemical Aspects of Hydrogen Transfer*; Hynes, J.; Limbach, H.-H., Eds.; Wiley-VCH: Weinheim, 2006. (m) Hatcher, E.; Soudackov, A.; Hammes-Schiffer, S. *J. Am. Chem. Soc.* **2007**, *129*, 187.
- (13) Stuchebrukhov, A. A.; Georgievskii, Y. *J. Chem. Phys.* **2000**, *113*, 10438.
- (14) (a) Vorotyntsev, M. A.; Dogonadze, R. R.; Kuznetsov, A. M. *Dokl. Akad. Nauk SSSR* **1973**, *209*, 1135. (b) Kuznetsov, A. M.; Ulstrup, J. *Can. J. Chem.* **1999**, *77*, 1085.
- (15) Costentin, C.; Robert, M.; Savéant, J.-M. *J. Electroanal. Chem.* **2006**, *588*, 197.

**Table 1.** Apparent Standard Rate Constants for the Electrochemical Oxidation of **1**

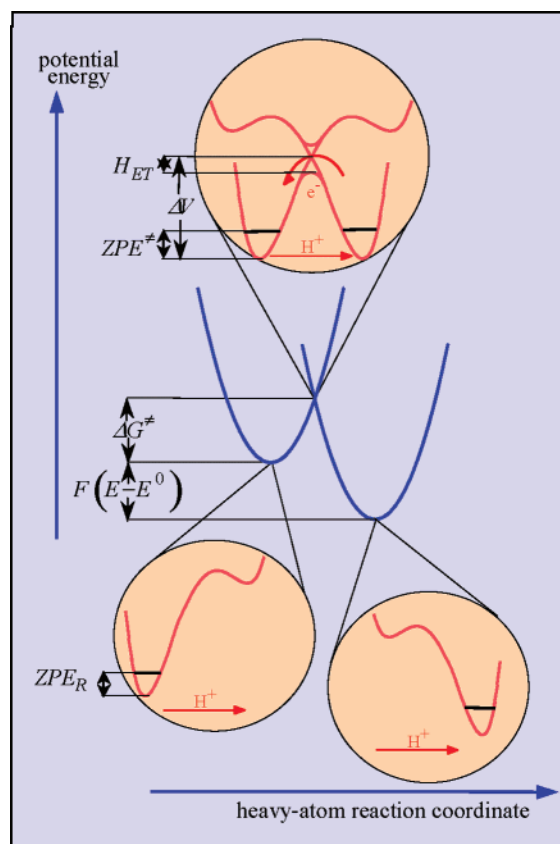
temp (°C)	$D$ ( $\times 10^5$ cm <sup>2</sup> s <sup>-1</sup> )	$k_{S,H}^{ap}$ ( $\times 10^3$ cm s <sup>-1</sup> )	$k_{S,D}^{ap}$ ( $\times 10^3$ cm s <sup>-1</sup> )	$k_{S,H}^{ap}/k_{S,D}^{ap}$
21.5	1.25	8	5	1.6
10	1.0	5.5	3	1.8
0	0.9	2.5	2	1.25
-10	0.8	1.5	0.85	1.8
-20	0.6	0.7	0.5	1.4

**Figure 2.** Arrhenius plots for the oxidation of **1** in the absence (red data points) and presence of 2% CD<sub>3</sub>OD (blue data points).**Scheme 2**

introducing the standard potential,  $E^0$ , the apparent (uncorrected from double-layer effects) standard rate constant,  $k_S^{ap}$ . The transfer coefficient,  $\alpha$ , is likely to be close to 0.5, in view of the fact that the system is not far from reversibility, even at the lowest temperatures. The subscript “0” means that the concentrations are those at the surface of the electrode.  $I$  is the current density and  $F$  the Faraday constant. The values of  $k_S^{ap}$  can be derived from the anodic-to-cathodic peak separation.<sup>17</sup> Simulations<sup>18</sup> of the voltammograms, shown in Figure 1 and Figure 1S in the Supporting Information, allow the determination of  $k_S^{ap}$  and the diffusion coefficient,  $D$ , since the dimensionless current–potential response,  $\psi(\xi)$  (with  $\psi = I/FC^0\sqrt{D}\sqrt{\alpha Fv/RT}$  and  $\xi = (\alpha F/RT)(E - E^0)$ , where  $C^0$  is total concentration and  $v$  is scan rate), is a function of a single dimensionless parameter,  $k_S^{ap}\sqrt{RT/\alpha FvD}$ .<sup>17</sup> Taking  $\alpha = 0.5$ , the ensuing values of  $k_S^{ap}$  are listed in Table 1. Figure 2 show the Arrhenius plots derived from the values in Table 1.

**1.2. Rate Law and Linearized Rate Law: Expression of the Standard Rate Constant.** How can we justify the use of the Butler–Volmer rate law and estimate the two parameters—reorganization energy and pre-exponential factor—that govern the kinetics? These are the next questions we discuss.

Analysis of the CPET reaction requires considering the four diabatic states represented in Scheme 2. These four diabatic states may be mixed into two states that are adiabatic toward

**Figure 3.** Schematic representation of the potential energy profiles in the case where the CPET reaction involves only the proton vibrational ground states.

proton transfer, as shown in the upper inset of Figure 3: the high-energy  $^-\text{OArHN}^{*+}$  state is mixed with the stable  $\text{HOArN}^{*+}$  state, and the high-energy  $\text{ArOH}^{*+}$  state is mixed with the stable  $\text{ArO}^*\text{HN}^{*+}$  state, assuming that the proton transfer is electronically adiabatic.

Based on the Born–Oppenheimer approximation, which takes into account that both electrons and protons are light particles compared to the other atoms in the system, their transfer requires reorganizing solvent and heavy atoms to reach a transition state where both reactants and products have the same configuration. The electron being a much lighter particle than the proton, a second Born–Oppenheimer approximation implies that the electron is transferred at the avoided crossing intersection of the potential energy profiles of the resulting two states, while the proton tunnels through the barrier thus formed, leading to the potential energy profiles sketched in Figure 3. The representation there exemplifies a proton transfer occurring between two proton vibrational ground states. In a first simplified approach, we indeed consider that this is the most important contribution to the rate constant, as compared to transfers involving proton vibrational excited states. This point will be discussed later.

Within this framework, in the rate law relating the current density to the electrode potential,

$$\frac{I}{F} = -k(E) \left\{ [\mathbf{1}]_0 - \exp\left[-\frac{F}{RT}(E - E^0)\right] [\mathbf{1}^{*+}]_0 \right\} \quad (2)$$

the potential-dependent rate constant,  $k(E)$ , can be expressed, provided only the Fermi-level electron electronic states in the

(17) Savéant, J.-M. *Elements of Molecular and Biomolecular Electrochemistry*; Wiley-Interscience: Hoboken, NJ, 2006.

(18) Using the DigiElch software; see: Rudolph, M. J. *Electroanal. Chem.* **2003**, *543*, 23.



electrode are taken into account, as the product of a pre-exponential factor,  $Z$ , by the classical quadratic Marcus–Hush term related to the harmonic approximations sketched in Figure 3 (potentials in volts and energies in electronvolts):

$$k(E) = Z \exp\left[-\frac{\lambda}{4RT}\left(1 - \frac{F(E - E^0)}{\lambda}\right)^2 - \frac{\Delta ZPE}{RT}\right] \quad (3)$$

where  $\lambda$  is the reorganization energy of the heavy atoms during the reaction, and  $\Delta ZPE = ZPE^\ddagger - ZPE_R$  is the difference between the transferring proton zero-point energies at the transition state and at the reactant state. The pre-exponential factor,  $Z = Z_{el}\chi$ , is the product of the collision frequency,  $Z_{el} = \sqrt{RT/2\pi M}$  (where  $M$  is the reactant molar mass) and the transmission coefficient  $\chi$ ,

$$\chi = \frac{2p}{1+p} \quad (4)$$

where  $p$  is the probability of proton tunneling and electron transfer, which occurs at the transition state as sketched in the upper inset of Figure 3.  $p$  is obtained from the Landau–Zener expression:

$$p = 1 - \exp\left(-\pi\left(\frac{C}{RT}\right)^2 \sqrt{\frac{\pi RT}{\lambda}}\right) \quad (5)$$

The constant  $C$  measures the coupling between the reactant and product proton vibrational states.

A modeling of the barrier allowing an estimation of  $C_{eq}$  (i.e., the coupling constant corresponding to the equilibrium distance between the proton donor and acceptor atoms, here the oxygen and nitrogen atoms) as a function of the barrier height,  $\Delta V$ , depending on the distance between the donor and acceptor atoms,  $Q$ , will be presented in the next section.

In the general case where the electron transfer is not necessarily adiabatic, application of the Landau–Zener approximation to the electron transfer leads to eq 6:<sup>13</sup>

$$C_{eq} = \kappa C_{eq}^{ad} \quad (6)$$

with  $\kappa$  being the electronic transmission factor. We continue the discussion in the case where electron transfer is adiabatic, i.e.,  $\kappa = 1$ .

The degree of adiabaticity of the global CPET reaction is defined through eq 5: when the coupling constant  $C$  is large,  $p \rightarrow 1$ , and the reaction is adiabatic; when  $C$  is small, the reaction is non-adiabatic and  $p \rightarrow (\pi/RT)^{3/2}C^2/\sqrt{\lambda}$ .

In fact, mere consideration of the equilibrium coupling constant is not sufficient for an accurate description of the reaction kinetics.<sup>12i–k</sup> The actual coupling constant,  $C$ , being a function of the distance between the donor and acceptor atoms,  $Q$ , proton tunneling between the reactant and product states is a function of the donor–acceptor vibration (the shorter the distance, the easier proton tunneling). In a classical mechanical description, the contribution of each distance  $Q$  to proton tunneling is obtained by weighting the transmission coefficient (eq 4) by the Boltzmann probability  $P(Q)$  that the donor and acceptor atoms be at a distance  $Q$  from one another:

$$\chi = \int_{-\infty}^{+\infty} \chi(Q) P(Q) dQ \quad (7)$$

where  $P(Q)$  is the normalized Boltzmann distribution function for a classical harmonic oscillator,

$$P(Q) = \sqrt{\frac{f_Q}{2\pi RT}} \exp\left(-\frac{f_Q(Q - Q_{eq})^2}{2RT}\right) \quad (8)$$

and  $f_Q = 4\pi^2\nu_Q^2m_Q$  (where  $\nu_Q$  is frequency and  $m_Q$  is reduced mass).

In this averaging procedure, the effects of dynamical coupling between fluctuations of the  $Q$  coordinate and the coupling constant are regarded as negligible.<sup>12j</sup> This approximation has been shown to be justified for homogeneous CPET in the non-adiabatic limit<sup>12i,k,m</sup> (see also Supporting Information). It seems reasonable to assume that it is also applicable up to the adiabatic limit and for electrochemical reactions as well.

Up to this point, the potential-dependent rate constant,  $k(E)$ , in rate law (2) is given by a Marcus quadratic expression (eq 3), applied to the Fermi-level electron electronic states in the electrode. A more accurate description of the kinetics of the electrochemical reaction requires taking into account all electronic states of the electrons in the electrode, along the same lines as for outer-sphere and dissociative electron transfers, leading to a somewhat knotty-looking expression of the overall rate law.<sup>19</sup> However, considering the fact that the potential excursion in a cyclic voltammetric experiment (or in other electrochemical techniques) does not exceed a few hundred millivolts, the rate law may be linearized (see Supporting Information), leading to the applicability of rate law (1) and to the following equation defining the apparent standard rate constant:

$$k_S^{ap} \approx [\chi Z_{el}] \left[ \sqrt{\frac{\pi RT}{4F\lambda}} \exp\left(-\frac{\lambda}{4RT}\right) \right] \exp\left[-(\alpha + z_R)\frac{F\phi_S}{RT}\right] \exp\left(-\frac{\Delta ZPE}{RT}\right) \quad (9)$$

or

$$k_S^{ap} = \chi \frac{RT}{2\sqrt{2M\lambda}} \exp\left(-\frac{\lambda}{4RT}\right) \exp\left[-(\alpha + z_R)\frac{F\phi_S}{RT}\right] \exp\left(-\frac{\Delta ZPE}{RT}\right)$$

where  $z_R$  is the charge of the reactant and  $\phi_S$  is the potential difference between the reaction site and the solution. The value of the transfer coefficient,  $\alpha$ , is considered as constant (but not necessarily equal to 0.5) over the relatively narrow potential excursion in standard cyclic voltammetric experiments.

We note that, if the CPET reaction is fully adiabatic, i.e., if  $\chi \approx 1$  (and  $p \approx 1$ ), the H/D kinetic isotope effect is expected to be small since it merely results from the variation of  $\Delta ZPE$  from hydrogen to deuterium:

$$\frac{k_{S,H}^{ap}}{k_{S,D}^{ap}} = \exp\left[\frac{-\Delta ZPE_H + \Delta ZPE_D}{RT}\right] \quad (10)$$

Since in standard treatments,<sup>20</sup>  $\Delta ZPE_D \approx \Delta ZPE_H/\sqrt{2}$ :

$$k_{S,H}^{ap}/k_{S,D}^{ap} = \exp[(\Delta ZPE_H/RT)(1/\sqrt{2} - 1)]$$

Larger values of the H/D kinetic isotope effect are expected when non-adiabaticity increases ( $\chi < 1$  and  $p < 1$ ), since in addition to the decrease of  $\Delta ZPE$  from hydrogen to deuterium, tunneling is expected to be slower in the latter case than in the former.

**1.3. Application to the Oxidation of Compound 1.** The preceding section justifies our treatment of the experimental data by means of the Butler–Volmer rate law and of Arrhenius plots in the form displayed in Figure 2, i.e., taking into account that  $z_R = 0$ :

$$\ln\left(\frac{k_S^{\text{ap}}}{T}\right) = \ln \chi + \ln\left(\frac{R}{2\sqrt{2M\lambda}}\right) - \left[\frac{\lambda}{4} + \alpha F\phi_S + \Delta\text{ZPE}\right] \frac{1}{RT} \quad (11)$$

A preliminary study of **1** pointed to a non-adiabatic CPET.<sup>8a</sup> However, this study was based on a single temperature analysis. Moreover, data analysis was carried out using non-adiabatic formulas for the coupling constant, which may not be appropriate. A first clue that the electrochemical CPET oxidation of **1** is, in fact, adiabatic is provided by the smallness of the H/D kinetic isotope effect (Table 1):  $1.6 \pm 0.2$ . This is confirmed by the fact that the data in Figure 2 could not be fitted with values of  $\chi$  smaller than 1.

From the slope of the Arrhenius plots in Figure 2,

$$\frac{\lambda}{4} + \alpha F\phi_S + \Delta\text{ZPE} = 0.285 \text{ eV (for H)}, \quad 0.297 \text{ eV (for D)}$$

Since the cyclic voltammetric response is close to reversibility,  $\alpha$  can be taken as equal to 0.5. The potential  $\phi_S$  is estimated to be 0.12 V.<sup>21</sup> Using  $k_{S,H}^{\text{ap}}/k_{S,D}^{\text{ap}} = \exp[(\Delta\text{ZPE}_H/RT)(1/\sqrt{2} - 1)] = 1.6$ ,  $\Delta\text{ZPE}_H$  can be estimated as equal to  $-0.04$  eV. The value of the reorganization energy ensues:  $\lambda = 1.06$  eV.

This rather modest value of the reorganization energy may be rationalized as follows.  $\lambda$  has an intramolecular contribution,  $\lambda_i$ , and a solvent reorganization contribution,  $\lambda_0$ . As shown earlier,<sup>15</sup>  $\lambda_0$  may itself be decomposed into two contributions, one relative to electron transfer,  $\lambda_0^{\text{ET}}$ , and the other to proton transfer,  $\lambda_0^{\text{PT}}$ :

$$\lambda_0^{\text{ET}} = \frac{e^2}{4\pi\epsilon_0} \left( \frac{1}{\epsilon_{\text{op}}} - \frac{1}{\epsilon_S} \right) \frac{1}{2a} \quad (12)$$

$$\lambda_0^{\text{PT}} = \frac{1}{4\pi\epsilon_0} \left[ \left( \frac{\epsilon_S - 1}{2\epsilon_S + 1} \right) - \left( \frac{\epsilon_{\text{op}} - 1}{2\epsilon_{\text{op}} + 1} \right) \right] \frac{(\mu_R - \mu_P)^2}{a^3} \quad (13)$$

$\epsilon_0$  is the vacuum permeability, and  $\epsilon_{\text{op}}$  ( $= 2$ ) and  $\epsilon_S$  ( $= 36.6$ ) are the optical and static dielectric constants of the solvent.  $a$  ( $= 4.78$  Å), the radius of the reactant equivalent sphere, is derived from quantum chemical calculation of the reactant optimized geometry. The dipole moments of the reactant and product are derived from similar calculations:  $\mu_R = 3.43$  D and  $\mu_P = 9.65$  D. It follows that  $\lambda_0^{\text{ET}} = 0.713$  eV and  $\lambda_0^{\text{PT}} = 0.062$  eV.

$\lambda_i$  may be estimated as follows.  $Y$  is taken as the index of the reaction progress, varying between 0 and 1. Each coordinate of the molecule,  $R_j$ , is assumed to vary linearly from its value in the reactant,  $R_{j,Y=0}$ , to its value in the product,  $R_{j,Y=1}$ :

$$R_j(Y) = R_{j,Y=0} + (R_{j,Y=1} - R_{j,Y=0})Y$$

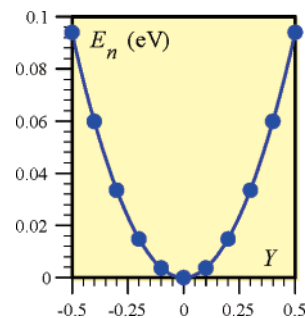


**Figure 4.** Determination of the intramolecular reorganization energy (see text).

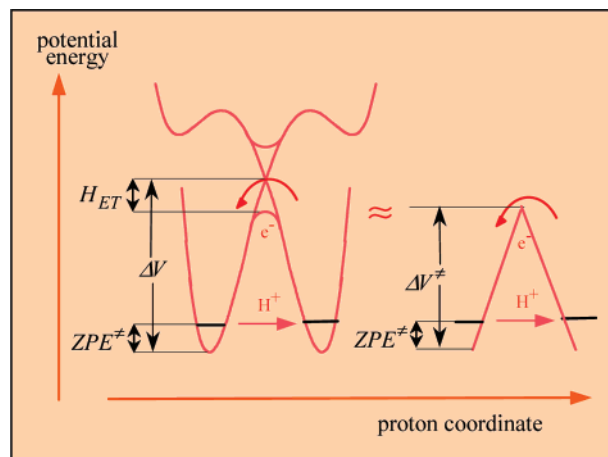


**Figure 5.** Modeling of the proton tunneling barrier. Triangular approximation.

Once all the  $R_{j,Y=0}$  and  $R_{j,Y=1}$  values have been determined by geometry optimization of the reactant and product structures, the energy of the system is calculated for a series of increasing values of  $Y$ , leading to the quadratic variation shown in Figure 4,  $E_n = \lambda_i Y^2$ , thus leading to  $\lambda_i = 0.375$  eV. It is interesting to note that  $\lambda_i = 0.2$  eV for the C–OH/C–OH<sup>+</sup> reaction and  $\lambda_i = 0.06$  eV for the C–O<sup>−</sup>/C–O<sup>•</sup> reaction. Concerning intramolecular reorganization, the price to pay for the benefit of the thermodynamic advantage offered by CPET reaction is thus rather modest, namely 175 meV in terms of intrinsic barrier, i.e., a factor of 0.2 in terms of rate constant as compared to the C–OH/C–OH<sup>+</sup> reaction, and 315 meV in terms of intrinsic barrier, i.e., a factor of 0.05 in terms of rate constant as compared to the C–O<sup>−</sup>/C–O<sup>•</sup> reaction.

In total,  $\lambda = \lambda_0^{\text{ET}} + \lambda_0^{\text{PT}} + \lambda_i = 1.15$  eV, a value that agrees with the experimental value (1.06 eV) in a manner that is quite satisfactory in view of the various approximations included in the theoretical treatment.

We now attempt to interpret the fact that the CPET reaction is adiabatic. As described in the previous section, adiabaticity is measured by the value of the transmission coefficient  $\chi$ , and hence that of the coupling constant  $C$ . Assuming that adiabatic proton potential profile,  $V(q,Q)$ , is a symmetrical double well (Figure 5), the coupling between the two electronic states can be calculated by the following

(19) (a) Levich, V. G. Present State of the Theory of Oxidation–Reduction in Solution (Bulk and Electrode Reactions). In *Advances in Electrochemistry and Electrochemical Engineering*; Delahay, P., Tobias C. W., Eds.; Wiley: New York, 1955; pp 250–371. (b) Gosavi, S.; Marcus, R. A. *J. Phys. Chem. B* **2000**, *104*, 2057. (c) Reference 17, pp 39, 40, 368–370. (d) Savéant, J.-M. *J. Phys. Chem. B* **2002**, *106*, 9387.

(20) Melander, L. *Isotope Effects on Reaction Rates*; Ronald Press Co.: New York, 1960.

(21) Meneses, A. B.; Antonello, S.; Arévalo, M. C.; Maran, F. *Electroanalysis* **2006**, *18*, 363.

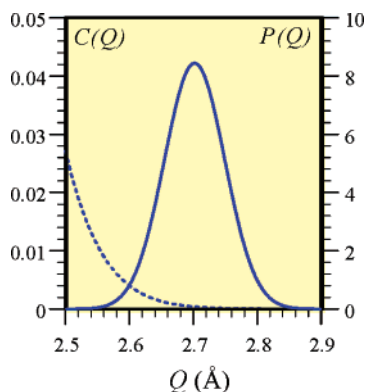


**Figure 6.** Boltzmann proton donor–acceptor distance distribution (solid line) and coupling constant as a function of the proton donor–acceptor distance (dotted line).

semi-classical formula for an electronically adiabatic proton transfer:<sup>22</sup>

$$C(Q) = hv_0^\ddagger \exp\left[-\frac{2\pi}{h} \left( \int_{q_i}^{q_f} \sqrt{2m_p(V(q,Q) - E)} dq \right)\right] \quad (14)$$

where  $\nu_0^\ddagger$  is the proton well frequency,  $E = hv_0^\ddagger/2$  is the energy level,  $m_p$  is the proton mass, and  $q_i$  and  $q_f$  are the classical turning points in each well at fixed  $Q$ . The proton-tunneling barrier may be approximated by an isosceles triangle, as shown in Figure 5 (see also Supporting Information). Classical turning points are proton positions corresponding to a potential energy equal to  $hv_0^\ddagger/2$ .

Within this model, the coupling constant is (see Supporting Information)

$$C(Q) = hv_0^\ddagger \exp\left[-\frac{8\sqrt{2}}{3} \sqrt{\frac{hv_0^\ddagger}{\Delta V^\ddagger}} \left(\frac{\Delta V^\ddagger}{hv_0^\ddagger} - \frac{1}{2}\right)^{3/2}\right] \quad (15)$$

with

$$\Delta V^\ddagger(Q) = \frac{f_0^\ddagger}{4} \left( \frac{Q - d_{\text{NH}}^0 - d_{\text{OH}}^0}{2} \right)^2 \quad (16)$$

where  $f_0^\ddagger = 4\pi^2\nu_0^{\ddagger 2}m_p$  is the force constant of the proton well and  $d_{\text{OH}}^0$  and  $d_{\text{NH}}^0$  are the proton equilibrium distances in the reactant and product, respectively.

Averaging of the transmission coefficient in the classical mechanical  $Q$  motion limit through eqs 7 and 8 requires estimation of the proton donor–acceptor vibration frequency,  $\nu_Q$ , and of the reduced mass associated with this vibration,  $m_Q$ . It finally comes out that estimation of the averaged transmission coefficient requires the values of a limited number parameters,  $\nu_Q$ ,  $\nu_0^\ddagger$ ,  $Q_{\text{eq}}$ ,  $d_{\text{OH}}^0$ , and  $d_{\text{NH}}^0$ . Those parameters can be evaluated as follows: equilibrium hydrogen–oxygen or hydrogen–nitrogen distances,  $d_{\text{OH}}^0$  and  $d_{\text{NH}}^0$ , can be taken as 0.96 and 1 Å, respectively;<sup>23</sup> equilibrium distance  $Q_{\text{eq}}$  is estimated from a combination of structural data (X-ray crystal structure) on compound **2**<sup>3c</sup> and ab initio calculation, leading to 2.7 Å;<sup>24</sup> the proton donor–acceptor frequency is calculated as  $h\nu_Q = 0.08$  eV (see Supporting Information);  $\nu_0$  in the reactant structure is calculated as 3260  $\text{cm}^{-1}$  (see methodology for quantum chemi-

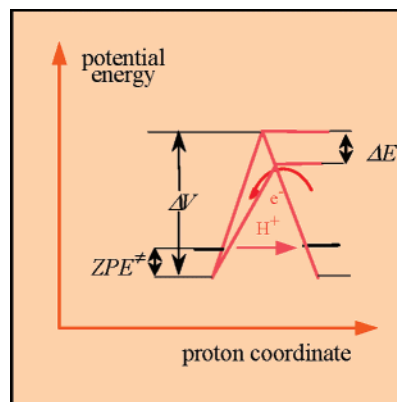


**Figure 7.** Modeling of electric field effect on the proton tunneling barrier.

cal calculation), which is a typical value for an O–H vibration that is strongly hydrogen-bonded.<sup>25</sup> The frequency of interest is the corresponding frequency in the transition state,  $\nu_0^\ddagger$ , obtained from  $\Delta\text{ZPE} = (h\nu_0^\ddagger - h\nu_0)/2 = -0.04$  eV. Therefore, we consider  $h\nu_0^\ddagger \approx 0.3$  eV. With these parameters, the transmission coefficient is evaluated using eqs 4, 5, 7, 8, 15, and 16:  $\chi = 0.004$ . The contribution of  $Q$  distances shorter than the equilibrium distance strongly impacts the magnitude of the transmission coefficient, since they involve higher coupling constants (Figure 6). Indeed, with the sole equilibrium  $Q$  distance, the transmission coefficient would be  $\chi_{\text{eq}} = 0.00043$ .

The averaged value is much smaller than unity, in contradiction with experimental data. However, as will be seen later, the evaluated value,  $\chi = 0.004$ , is in agreement with a transmission coefficient derived from homogeneous experiments on compound **2** (see section 2,  $0.07 \times 10^{-2} < \chi < 1.2 \times 10^{-2}$ ). Moreover, it should be remembered that the electrochemical reaction takes place in a strong electric field, of the order of  $10^7$   $\text{V cm}^{-1}$ , leading to the stabilization of the zwitterionic form in the transition state, thus decreasing the proton tunneling barrier. This stabilization energy is estimated from the stabilization energy of a dipole in a parallel electric field. Assuming that the reactant is close to the electrode, i.e., located at a distance  $a = 4.78$  Å from the electrode, the stabilization energy  $\Delta E$  of the zwitterionic form, described as the dipole with opposite elementary charge separated by a distance  $Q$ , is calculated:

$$\Delta E = \frac{Q}{a} F(E_p - \phi_s)$$

where  $E_p$  is the peak potential in cyclic voltammetry experiments.

We then introduce this stabilization energy in the model presented above in such a manner that the activation energy in the presence of an electric field is  $\Delta V^\ddagger(Q) - \Delta E(Q)$ . This is achieved through a modification of the slope of the segment describing the reactants' diabatic proton profile

(23) *Handbook of Chemistry and Physics*, 81st ed.; CRC Press: Boca Raton, FL, 2000; pp 9–10.

(24) Since the three atoms O, H, and N are not collinear, the  $Q$  coordinate is not the actual O–N distance but the sum of O–H and H–N distances that is approximatively constant upon proton displacement (see quantum mechanical calculation section).

(25) Rostkowska, H.; Nowak, M. J.; Lapinski, L.; Adamowicz, L. *Phys. Chem. Phys. Chem.* **2001**, 3, 3012.

(22) Child, M. S. *Molecular Collision Energy*; Academic Press: New York, 1974.

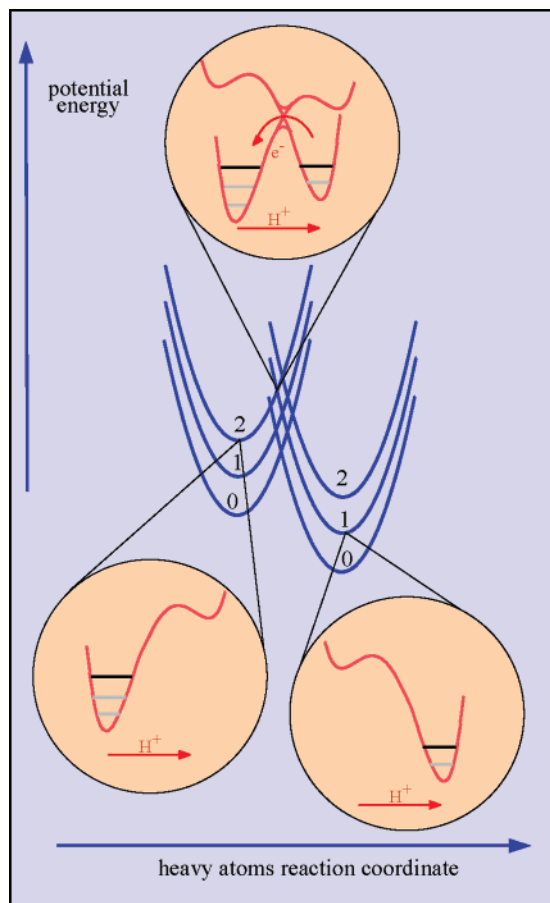


**Figure 8.** Schematic representation of the potential energy profiles in the case where the CPET reaction involves proton vibrational excited states. In the above example, the proton is transferred from state  $\mu = 2$  to state  $\nu = 1$ .

(Figure 7). The coupling constant in the presence of an electric field is thus given by (see Supporting Information)

$$C_{\text{ef}}(Q) = hv_0 \exp \left\{ -\frac{2\sqrt{2}}{3} \frac{f_0^\ddagger}{hv_0^\ddagger} \left[ \sqrt{B} \left( q^\ddagger - d_{\text{OH}}^0 - \frac{hv_0^\ddagger}{2B} \right)^{3/2} + \sqrt{A} \left( Q - q^\ddagger - d_{\text{NH}}^0 - \frac{hv_0^\ddagger}{2A} \right)^{3/2} \right] \right\} \quad (17)$$

where

$$A = \frac{f_0^\ddagger}{8} (Q - d_{\text{NH}}^0 - d_{\text{OH}}^0), \quad B = A \frac{(\Delta V^\ddagger - \Delta E)}{(\Delta V^\ddagger + \Delta E)},$$

$$q^\ddagger = \frac{A(Q - d_{\text{NH}}^0) + Bd_{\text{OH}}^0}{A + B}$$

Averaging over  $Q$  distances in the classical mechanical limit for  $Q$  motion leads to  $\chi = 0.3$ , showing that the reaction is close to being adiabatic, even though  $\chi$  has not reached unity. This difference is not very surprising in view of the various approximations embodied in the theoretical treatment and in parameter estimates.

**1.4. Involvement of Proton Vibrational Excited States.** So far, we have considered only the case where proton transfer occurs between two proton vibrational ground states. What is the effect of taking into account the possibility that proton

transfer involves proton vibrational excited states? That is the question we address now. Such a situation is exemplified in Figure 8, which shows a case where proton transfer occurs between the vibrational excited states  $\mu = 2$  and  $\nu = 1$ . As compared to the transfer from state  $\mu = 0$  to state  $\nu = 0$ , the situation is more favorable in terms of both driving force and proton tunneling. The corresponding contribution has, however, to be weighted by the Boltzmann probability of the system being in this excited state. In a general manner, the rate constant appears as a sum of a series of individual rate constants,  $k_{\mu\nu}$ , contributing each according to its Boltzmann weight:

$$k(E) = \frac{\sum_{\mu=0}^{\infty} \sum_{\nu=0}^{\infty} k_{\mu\nu}(E) \exp(-\mu hv_0/RT)}{\sum_{\mu=0}^{\infty} \exp(-\mu hv_0/RT)} \quad (18)$$

where  $\nu_0$  is the frequency of the H vibration, assumed to be the same in the transition reactant and product electronic states.  $k_{\mu\nu}$  is, after linearization (see Supporting Information), with

$$k_{\mu\nu}(E) = Z_{\text{el}} \sqrt{\frac{RT}{4\pi\lambda}} \pi \exp\left(-\frac{\lambda}{4RT}\right) \chi_{\mu\nu} \exp\left[-(\alpha_{\mu\nu} + z_{\text{R}}) \frac{F\phi_{\text{S}}}{RT}\right] \times \exp\left(\frac{-(2\mu + 1) \Delta\text{ZPE}}{RT}\right) \exp\left[\frac{\alpha_{\mu\nu} F(E - E_{\mu\nu}^0)}{RT}\right] \quad (19)$$

$$F E_{\mu\nu}^0 = F E_{00}^0 + (\nu - \mu) hv_0 \quad (E_{00}^0 \approx E^0) \quad (20)$$

$\alpha_{\mu\nu}$  can be considered as constant, having the same value whatever  $\mu$  and  $\nu$  along the cyclic voltammetric wave ( $\alpha_{\mu\nu} = \alpha$ ). It follows that the Butler–Volmer rate law (eq 2) is applicable and that the overall standard rate constant can be expressed as

$$k_{\text{S}}^{\text{ap}} = \chi Z_{\text{el}} \sqrt{\frac{RT}{4\pi\lambda}} \pi \exp\left(-\frac{\lambda}{4RT}\right) \exp\left[-(\alpha_{\mu\nu} + z_{\text{R}}) \frac{F\phi_{\text{S}}}{RT}\right] \exp\left(\frac{-\Delta\text{ZPE}}{RT}\right) \quad (21)$$

with

$$\chi = \frac{\sum_{\mu} \sum_{\nu} \left\{ \chi_{\mu\nu} \exp\left[-\alpha \frac{(\nu - \mu) hv_0}{RT}\right] \exp\left(-\frac{\mu hv_0}{RT}\right) \exp\left(\frac{-2\mu \Delta\text{ZPE}}{RT}\right) \right\}}{\sum_{\mu=0}^{\infty} \exp\left(-\frac{\mu hv_0}{RT}\right)} \quad (22)$$

Assuming that  $\chi_{00} = 1$ , as earlier from experimental data, all the other  $\chi_{\mu\nu} = 1$  since they involve proton tunneling through smaller barriers. Application of eq 22 (with  $hv_0 = 0.4$  eV and  $\Delta\text{ZPE} = -0.04$  eV as calculated earlier) leads to  $\chi = 1.01$ , showing that the contribution of the proton excited vibrational states is negligible, thus validating the discussion and conclusions in section 1.3. Taking  $\chi_{00} = 0.30$ , as derived from the model, and all the other  $\chi_{\mu\nu} = 1$ , application of eq 22 leads to



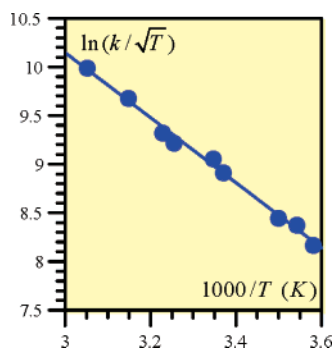


**Figure 9.** Arrhenius plots for the oxidation of **2** in acetonitrile by a series of triarylamine cation radicals, from the data in ref 3c.

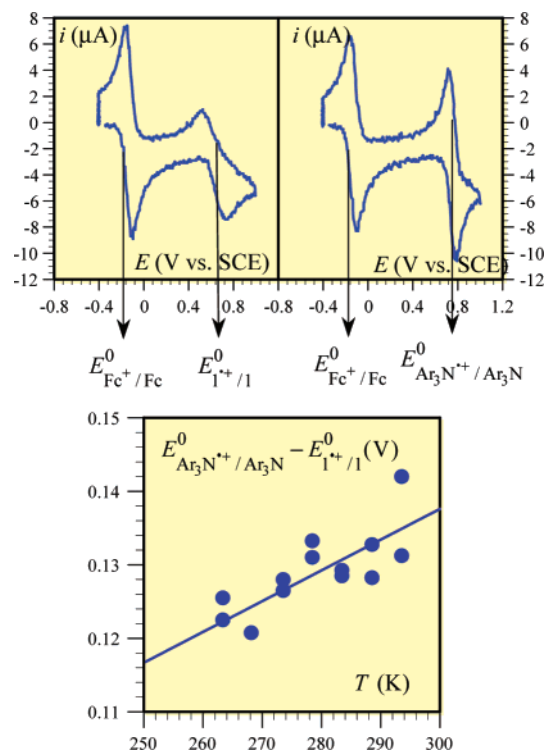


**Figure 10.** (Top) Cyclic voltammograms at 0 °C of (left) decamethylferrocene (1.6 mM) + **1** (1.53 mM) and (right) decamethylferrocene (1.6 mM) + tritolyamine (1.52 mM). (Bottom) Variation of the driving force with temperature.

$\chi = 0.31$ , again showing a negligible contribution of the proton excited vibrational states.

## 2. Homogeneous Oxidation of Compound 2.

**2.1. Variations of the Kinetics and Driving Force with Temperature.** The variation of the rate constant of CPET from **2** to a series of triarylamine cation radicals, previously obtained by Mayer et al.,<sup>3c</sup> is displayed in Figure 9 as an Arrhenius plot of the same form as in Figure 2. Analysis of these results requires knowing the variation of the driving force of the reaction,  $\Delta G^0 = F(E_{A^{+}/A}^0 - E_{2^{+}/2}^0) = \Delta H^0 - T\Delta S^0$  ( $A = \text{trip-tolylamine}$ ) with temperature, leading to the standard entropy,  $\Delta S^0$ . The structures of **1** and **2** are very similar, and so are expected to be the values of  $\Delta S^0$  (this point will be further discussed in section 2.3). We may thus derive the value of  $\Delta S^0$  from the variation with temperature of the difference in the standard potentials for the  $1^{+}/1$  and  $A^{+}/A$  couples obtained from cyclic voltammetric experiments. Since the two standard

potentials are very close to one another, the cyclic voltammetric waves for these two couples are expected to overlap each other, making the determination of their standard potentials difficult. A more distant third couple, decamethylferrocenium/ decamethylferrocene, was thus used to circumvent this difficulty, as shown in Figure 10, leading to the temperature variations of interest reported in the lower part of Figure 10. Linear least-squares fitting of this variation led to

$$\Delta H^0 = -0.103 \pm 0.059 \text{ eV}^{26}$$

$$\Delta S^0 = -0.418 \pm 0.21 \text{ meV/K}$$

(For the determination of the errors on  $\Delta H^0$  and  $\Delta S^0$ , see the Experimental Section.)

**2.2. Linearized Rate Law: Arrhenius Plots.** In the homogeneous case, eq 3 is replaced by

$$k = \chi Z_{\text{hom}} \exp \left[ -\frac{\lambda}{4RT} \left( 1 - \frac{F(E_{A^{+}/A}^0 - E^0)}{\lambda} \right)^2 - \frac{\Delta ZPE}{RT} \right] \quad (23)$$

where  $E_{A^{+}/A}^0$  is the standard potential of the electron-acceptor couple.  $\lambda$  involves heavy-atom reorganization not only in the molecule that undergoes the CPET reaction but also in the electron-acceptor molecule.  $\chi$  is the transmission factor resulting from proton tunneling through the transition-state barrier, and  $Z_{\text{hom}} = N_A d^2 \sqrt{8\pi RT/M}$  (where  $d$  is the sum of the molecular reactant equivalent radii and  $M$  is the reduced mass).

Insofar as the range of standard potentials offered by the series of acceptors is not larger than a few hundred millivolts around the aminophenol standard potential,  $E^0$ , eq 23 can be linearized as

$$\ln k \approx \ln(\chi Z_{\text{hom}}) - \frac{1}{RT} \left[ \frac{\lambda}{4} - \frac{F}{2} (E_{A^{+}/A}^0 - E^0) \right] - \frac{\Delta ZPE}{RT} \quad (24)$$

Noting that

$$F(E_{A^{+}/A}^0 - E^0) = \Delta H^0 - T\Delta S^0$$

eq 24 may be recast under a form appropriate for Arrhenius plot analyses:

$$\ln \left( \frac{k}{\sqrt{T}} \right) = \ln \left( N_A \chi d^2 \sqrt{\frac{8\pi R}{M}} \right) - \frac{\Delta S^0}{2R} - \frac{\lambda/4 - \Delta H^0/2 + \Delta ZPE}{RT} \quad (25)$$

The reorganization energy,  $\lambda$ , and the transmission coefficient,  $\chi$ , can therefore be derived from the Arrhenius plot, provided  $\Delta H^0$  and  $\Delta S^0$  are known.

**2.3. Application to the Oxidation of Compound 2.** The data in Figure 9 can be fitted with the linear eq 25 (the middle of the electron-acceptor standard potential range is indeed close to the  $E^0$  of the CPET reaction), leading to

$$\ln(k/\sqrt{T}) = a - b/T$$

with  $a = 20.185 \pm 0.108$  and  $b = 3345 \pm 24 \text{ K}$ .

It follows that (with  $M = 164.8 \text{ g mol}^{-1}$ ,  $d = 9 \text{ \AA}$ , corresponding to  $Z_{\text{hom}} = 3 \times 10^{11} \text{ M}^{-1} \text{ s}^{-1}$ ,<sup>27</sup> and  $\Delta ZPE$

(26)  $\Delta H^0 = -0.103 \text{ eV}$  is obtained using  $\Delta G^0 = 0.02 \text{ eV}$  from ref 3c and  $\Delta S^0$  from Figure 10.

assumed to be the same as previously, i.e.,  $-0.04$  eV)

$$0.07 \times 10^{-2} < \chi < 1.2 \times 10^{-2}$$

and

$$\lambda = 0.79 \pm 0.12 \text{ eV}$$

From the experimental value of  $\chi$ , we conclude that the homogeneous CPET to **2** is non-adiabatic, whereas the electrochemical CPET to **1** is adiabatic. The estimated value obtained from the crude model discussed previously, i.e.,  $\chi = 0.4 \times 10^{-2}$ , is in agreement with experimental value, thus validating the conclusion. As a further test, we may come back to the appropriateness of deriving  $\Delta H^0$  and  $\Delta S^0$  for **2** from a  $\Delta S^0$  value derived from experiments carried out with **1** (section 2.1). We note that the electrochemical standard rate constants at room temperature for **2** and **1** are  $0.03^{3c}$  and  $0.08$  cm/s, respectively. A likely explanation of this small difference is that the solvation of **2**<sup>•+</sup> is a little stronger than for **1**<sup>•+</sup> because the charge is somewhat more concentrated, leading to a small increase of  $\lambda_0^{\text{ET}}$ , which makes the heterogeneous reorganization energy pass from 1.06 to 1.15 eV. If **2**<sup>•+</sup> is indeed a little more solvated than **1**<sup>•+</sup>,  $\Delta S^0$  for **2** should be slightly smaller than the value that we used in eq 20, resulting in a reinforcement of the conclusion that the CPET involving **2** is non-adiabatic. Another clue pointing to the same conclusion is that the H/D kinetic isotope effect is somewhat larger in the homogeneous case,  $2.6 \pm 0.4$ , than in the electrochemical case,  $1.6 \pm 0.2$ .

The reason for this difference in the degree of non-adiabaticity is related to the earlier observation that the adiabatic character of the electrochemical reaction is brought about by the stabilization of the reactant zwitterionic form by the double-layer electric field. A similar effect, due to the field generated by the charge borne on the electron acceptor, is likely to be less pronounced in the homogeneous case.

We analyze now the reorganization energy,  $\lambda$ , of the cross-exchange reaction between **2** and the electron acceptor A. The value of the self-exchange reorganization energy,  $\lambda_{2^{•+}/2}$ , of the CPET reaction is extracted from the value of  $\lambda$ , just measured, and  $\lambda_{A^{•+}/A}$  by application of the classical Marcus cross-exchange relationship:<sup>28</sup>

$$\lambda = \frac{\lambda_{2^{•+}/2} + \lambda_{A^{•+}/A}}{2}$$

where  $\lambda_{A^{•+}/A} = 0.5$  eV,<sup>29</sup> leading to  $\lambda_{2^{•+}/2} = 1.08$  eV.

This value of  $\lambda_{2^{•+}/2}$  is much smaller than the value, 2.3 eV, previously derived from the same experimental results.<sup>3c</sup> The reason for this discrepancy is the previous neglect of the variation of the driving force with temperature, which led to an overestimation of  $\lambda$  by  $\approx 0.61$  eV, and thus of  $\lambda_{2^{•+}/2}$  by  $\approx 1.22$  eV.

The reorganization energy of the self-exchange CPET reaction may finally be dissected into three contributions:

$$\lambda_{2^{•+}/2} = \lambda_{0,2^{•+}/2}^{\text{ET,hom}} + \lambda_{0,2^{•+}/2}^{\text{PT,hom}} + \lambda_{i,2^{•+}/2}$$

$\lambda_{i,2^{•+}/2}$  is the same as in the electrochemical case, i.e.,  $\lambda_{i,2^{•+}/2} \approx 0.375$  eV.  $\lambda_{0,2^{•+}/2}^{\text{PT,hom}}$  represents a small contribution that may

be approximately equated to the electrochemical value,  $\lambda_{0,2^{•+}/2}^{\text{PT,hom}} \approx 0.06$  eV. It follows that  $\lambda_{0,2^{•+}/2}^{\text{ET,hom}} \approx 0.65$  eV.

This value of the homogeneous solvent reorganization energy related to electron transfer, 0.65 eV, may be compared with its electrochemical counterpart, 0.82 eV. The outcome of the comparison is closer to the predictions of the Hush model ( $\lambda_{0,\text{self-exchange}}^{\text{ET,hom}} = \lambda_0^{\text{ET,el}}$ <sup>30</sup>) than to the Marcus model ( $\lambda_{0,\text{self-exchange}}^{\text{ET,hom}} = \lambda_0^{\text{ET,el}/2}$ <sup>28</sup>) of solvent reorganization in electrochemical electron-transfer reactions.

This conclusion falls in line with previous observations concerning the reduction of aromatic hydrocarbons in a similar aprotic solvent.<sup>31</sup>

**2.4. Involvement of Proton Vibrational Excited States.** The expression of the rate constant that takes into account the proton vibrational excited states is obtained by analogy to eq 18:

$$k = \frac{\sum_{\mu=0}^{\infty} \sum_{\nu=0}^{\infty} k_{\mu\nu} \exp\left(-\frac{\mu h\nu_0}{RT}\right)}{\sum_{\mu=0}^{\infty} \exp\left(-\frac{\mu h\nu_0}{RT}\right)} \quad (26)$$

with

$$k_{\mu\nu} = \chi_{\mu\nu} Z_{\text{hom}} \exp\left(-\frac{\Delta G_{\mu\nu}^{\ddagger}}{RT}\right) \quad (27)$$

where

$$\Delta G_{\mu\nu}^{\ddagger} = \frac{\lambda}{4} \left(1 - \frac{F(E_{A^{•+}/A}^0 - E^0) + (\mu - \nu)h\nu_0}{\lambda}\right)^2 + (2\mu + 1)\Delta\text{ZPE} \quad (28)$$

As seen before,  $\Delta\text{ZPE}$  is small relative to the other energies involved and may thus be neglected. We may also linearize the quadratic expression and consider that the transfer coefficient is close to 0.5 for each contribution to the rate constant. Then,

$$\Delta G_{\mu\nu}^{\ddagger} = \frac{\lambda}{4} - \frac{F(E_{A^{•+}/A}^0 - E^0) + (\mu - \nu)h\nu_0}{2} \quad (29)$$

$$k = \chi Z_{\text{hom}} \exp\left(-\frac{\lambda}{4RT} + \frac{F(E_{A^{•+}/A}^0 - E^0)}{2RT}\right) \quad (30)$$

where the global transmission coefficient,  $\chi$ , is expressed as

$$\chi = \frac{\sum_{\mu} \sum_{\nu} \left\{ \chi_{\mu\nu} \exp\left[-\frac{(\nu - \mu)h\nu_0}{2RT}\right] \exp\left(-\frac{\mu h\nu_0}{RT}\right) \right\}}{\sum_{\mu=0}^{\infty} \exp\left(-\frac{\mu h\nu_0}{RT}\right)} \quad (31)$$

(28) (a) Marcus, R. A. *J. Chem. Phys.* **1955**, *24*, 4955. (b) Marcus, R. A. *J. Chem. Phys.* **1955**, *43*, 579. (c) Marcus, R. A. *Electrochim. Acta* **1958**, *13*, 955.

(29) Sorensen, S. P.; Bruning, W. H. *J. Am. Chem. Soc.* **1973**, *95*, 2445.

(30) (a) Hush, N. S. *J. Chem. Phys.* **1958**, *28*, 952. (b) Hush, N. S. *Electrochim. Acta* **1958**, *13*, 1005.

(31) (a) See Figure 3 in ref 31b. (b) Kojima, H.; Bard, A. J. *J. Am. Chem. Soc.* **1975**, *97*, 6317.

(27) The  $d$  value ( $d$  is the sum of the molecular reactant equivalent radii), 9 Å, is in agreement with the radius calculated value, 4.78 Å.

In the framework of an *a fortiori* approach, the contributions of the proton vibrational excited states are maximized if we take for each of them the maximal value  $\chi_{uv} = 1$ . Then, for  $\chi_{00} = 0.004$ , we find that  $\chi = 0.0048$ , showing that the consideration of the proton vibrational excited states has only a modest impact on the kinetics of the reaction.

### Concluding Remarks

The one-electron oxidation of intramolecularly hydrogen-bonded phenols, such as the two compounds considered in the present study, offers a typical example of a CPET reaction, where the advantage over stepwise pathways thermodynamically offered by the concertedness of proton and electron transfers is achieved at the kinetic level. We have shown that the Marcus–Hush–Levich equations originally devised for electrochemical and homogeneous outer-sphere electron-transfer reactions are applicable to these CPET reactions, provided proton tunneling is duly taken into account in the expression of the rate constant pre-exponential factor, while solvent and intramolecular reorganization governs the intrinsic activation barrier. It also appears that the involvement of proton vibrational excited states is marginal as compared to that of the corresponding ground states. A further simplification, obtained from the linearization of the activation–driving force law, is valid in most practical circumstances. It allows the temperature dependence of the reaction kinetics to be treated by the classical Arrhenius plot analysis, which makes possible the separate determination of the pre-exponential factor and the reorganization energy. The pre-exponential factor is governed jointly by the degree of non-adiabaticity of the CPET and the standard entropy of the reaction. The latter quantity, as well as the standard enthalpy, can be derived from the variation of the driving force with temperature, as measured by the difference between the standard potentials of the donor and acceptor couples by, e.g., cyclic voltammetry. Ignorance or inaccurate determination of these two factors may lead to incorrect estimations of the degree of adiabaticity of the reaction and of the reorganization energy.

The kinetics of the homogeneous oxidation of aminophenol **2** by the tri-*p*-tolylamine cation radical revealed that it can be treated by the general Marcus formalism reaction, but not by its adiabatic version. Application of the above procedures indeed pointed to the conclusion that the reaction is non-adiabatic, with a transmission coefficient of the order of 0.004. It also led to a value of the reorganization energy of the cross exchange reaction that is more than half an electronvolt lower than a previous determination, in which the reaction was unduly regarded as adiabatic and the variation of the driving force with temperature was neglected.<sup>3c</sup> This is also the reason that the reorganization energy of the self-exchange CPET reaction was overestimated by ca. 1 eV. A further consequence is an overestimation of the intramolecular reorganization energy. A significant intramolecular reorganization does accompany the CPET reaction, but its energy cost is relatively modest, of the order of 0.4 eV, in line with quantum chemical estimations. It is, in fact, not much larger than the intramolecular reorganization energy characterizing the outer-sphere electron transfer that converts the aminophenol into its cation radical (0.2 eV). In other words, the assertion<sup>5</sup> that the main difference between outer-sphere electron transfers and CPET reactions relates to intramolecular reorganization rather than to the degree of adiabaticity is certainly not generally valid.<sup>32</sup>

Electrochemical one-electron oxidation of aminophenol **1**, which has characteristics very similar to those of aminophenol **2**, is adiabatic, in contrast with the homogeneous reaction, as revealed by the temperature dependence of its standard rate constant obtained from cyclic voltammetric experiments. We suggest that this difference in behavior is related to the fact that the electrochemical reaction takes place in a strong electric field that stabilizes the zwitterionic form of the reactant (in which the proton has been transferred from oxygen to nitrogen). Taking this difference in adiabaticity into account, the magnitudes of the reorganization energies of the two reactions appear to be quite compatible with one another, as revealed by an analysis of the solvent and intramolecular contributions in both cases.

### Experimental Section

**Chemicals.** Acetonitrile (Fluka, >99.5%, stored on molecular sieves), tri-*p*-tolylamine (Aldrich, 97%), the supporting electrolyte NBu<sub>4</sub>PF<sub>6</sub> (Fluka, puriss.) and CD<sub>3</sub>OD (Eurisco-top, 100%) were used as received.

2,4-Di-*tert*-butyl-6-(1-pyrrolidino)phenol (**1**) was synthesized following the procedure described by Maki et al.<sup>33</sup> A solution of 2,4-di-*tert*-butylphenol (3 mmol, Aldrich) in toluene (20 mL) was refluxed with pyrrolidine (3.6 mmol, Aldrich) and paraformaldehyde (3.9 mmol as formaldehyde, Aldrich). After being heated for 6 h, the solution was poured into water, and the organic portion was extracted with three portions of ethyl acetate. The combined organic layer was dried on magnesium sulfate. After removal of the solvent, the residue was purified by silica gel column chromatography and recrystallized from methanol.

**Instrumentation.** The working electrode was a 1-mm-diameter glassy carbon rod (Tokai) obtained by mechanical abrasion of an original 3-mm diameter rod. It was carefully polished and ultrasonically rinsed in absolute ethanol before use. The counter-electrode was a platinum wire and the reference electrode an aqueous SCE electrode. The electrode was pretreated *in situ* by means of several voltammetric cycles between  $-0.1$  V and the solvent/electrolyte cathodic discharge. The double-wall jacketed cell was thermostated by circulation of 2-propanol. The exact temperature inside the electrochemical cell was measured.

The potentiostat, equipped with positive feedback compensation and current measurer, was the same as previously described.<sup>34</sup> Ohmic drop was carefully compensated. The electrode area ( $= 0.0067$  cm<sup>2</sup>) was determined from the ferrocene oxidation peak current and the 7,7,8,8-tetracyanoquinodimethane (TCNQ, Aldrich) reduction peak current at low scan rate (0.5 V/s), knowing their diffusion coefficients in similar conditions.<sup>9,35</sup>

**Determination of the Errors in  $\Delta H^0$  and  $\Delta S^0$ .** The accuracy on  $\Delta S^0$  is given by  $\Delta S^0 = \Delta S_m^0 \pm ts$ , where  $t$  is determined by the Student's test with a 95% accuracy ( $t = 2.2$  for  $n = 14$  values) and  $s$  is determined as

$$s = \sqrt{\frac{\sum_{k=1}^n (\Delta G_k^0 - \Delta \hat{G}_k^0)^2}{n-2} \frac{n}{n \sum_{k=1}^n T_k^2 - \left( \sum_{k=1}^n T_k \right)^2}}$$

with  $\Delta \hat{G}_k^0$  being the value given by the linear regression for the  $k$ th data couple  $\Delta G_k^0$  and  $T_k$ . The accuracy on  $\Delta H^0$  is also given by  $\Delta H^0 =$

(32) The values of the global reorganization energy and of the degree of adiabaticity reported in refs 5 should be treated with caution since the variation of the driving force with temperature was not taken into account in the treatment of the Arrhenius plots.

(33) Maki, T.; Araki, Y.; Ishida, Y.; Onomura, O.; Matsumura, Y. *J. Am. Chem. Soc.* **2001**, *123*, 3371.

$\Delta H_m^0 \pm ts$ , where  $s$  is determined as

$$s = \sqrt{\frac{\sum_{k=1}^n (\Delta G_k^0 - \Delta \hat{G}_k^0)^2}{n-2} \frac{\sum_{k=1}^n T_k^2}{n \sum_{k=1}^n T_k^2 - \left( \sum_{k=1}^n T_k \right)^2}}$$

**Methodology for Quantum Chemical Calculation.** All *ab initio* calculations were performed with the Gaussian 98 series of programs.<sup>36</sup> We used the B3LYP method with a 6-31G\* basis set. To shorten the calculation time, computations were performed not on compound **1** or **2** but on a simpler molecule, 2-(1-pyrrolidino)phenol, where the *tert*-butyl groups were replaced by hydrogen atoms.

(34) Garreau, D.; Savéant, J.-M. *J. Electroanal. Chem.* **1972**, *35*, 309.

(35) Clegg, A. D.; Rees, N., V.; Klymenko, O. V.; Coles, B. A.; Compton, R. G. *J. Electroanal. Chem.* **2005**, *580*, 78.

(36) Frisch, M. J.; et al. *Gaussian 98*, Revision A.1; Gaussian, Inc.: Pittsburgh, PA, 1998.

The molecule's radius,  $a$ , is determined through a volume *ab initio* calculation<sup>37</sup> performed on the gas-phase optimized geometry. The O–H bond vibration frequency,  $\nu_0$ , is obtained from a frequency calculation on the gas-phase optimized geometry.

**Determination of  $Q_{\text{eq}}$ .** Potential energy profiles of the reactant (neutral compound) and product (cation radical) have been calculated as a function of the proton donor–acceptor distance,  $Q$ , defined as the sum of the O–H and H–N distances. Resulting equilibrium distances are very similar (close to 2.815 Å, as can be seen in Figure 4S, Supporting Information). Moreover, the calculated O–N distance is 2.72 Å, while the experimental value from structural data (X-ray crystal structure) of compound **2**<sup>3c</sup> is 2.6 Å. Therefore, we can estimate that a typical value for  $Q_{\text{eq}}$ , defined as the sum of the O–H and H–N distances, is 2.7 Å.

**Supporting Information Available:** Cyclic voltammograms and their simulations; derivation of the theoretical relationships; complete ref 36. This material is available free of charge via the Internet at <http://pubs.acs.org>.

JA071150D

(37) This keyword, available in Gaussian 98, requests that the molecular volume be computed, defined as the volume inside a contour of 0.001 electrons/bohr<sup>3</sup> density.